JOURNAL OF APPLIED POLYMER SCIENCE VOL. 19, PP. 1103–1117 (1975)

Crystallization of Macromolecular Domains

SHAUL M. AHARONI, *Allied Chemical Corporation, Chemical Research Center, Morristown, New Jersey 07960*

Synopsis

A theory is presented explaining the crystallization of polymers into thin and flat crystals or lamellae. Following the physical cluster theory, the internal and surface free energy of the "amorphous" macromolecular domain is described. Crystallization proceeds through an internal ordering of the domain, the attachment of the partially ordered domain onto a growth face, and, finally, regularization and domain deformation leading to minimization of both internal and surface free energy of the attached domain and its immediate neighborhood. The resultant fold surfaces comprise adjoining intact or deformed domes composed from proximal-reentry loops. Although arising from an adaptation of the physical cluster theory to describe the macromolecular domain, the free-energy equations controlling the crystallization process are essentially the same as those describing the primary nucleation in the prevailing crystallization theories. Segregation according to molecular weight is shown to arise from the size-dependent ability of the domains to improve their internal ordering. Lamellar thickening is shown to follow a critical-exponent equation dependent on surface free energy. Experimental data from the literature, corroborating the model, are presented.

INTRODUCTION

A Gaussian segmental density distribution of macromolecules in the melt or not-dilute solution, with the resultant high number of intermolecular "entanglements," stands in contradistinction to the rapid rate of crystallization such systems can manifest and the necessary high rate of "disentanglement" facilitating such crystallization. This high rate cannot be accomodated by the rather slow overall molecular mobility, reflected by the maximum relaxation time τ_m.

Therefore, a model was recently proposed by this author[1,2] in which a large number of the segments belonging to a macromolecule are uniformly packed in a macromolecular domain, and the rest of the segments extend beyond the domain proper. These segments interpenetrate the adjoining domains and account for the mechanical and rheological cohesion of the polymer. Our model is in agreement with the conclusions of Onogi and co-workers[3,4] based on rheological studies and with the conclusions of Lindenmeyer[5] drawn from thermodynamic considerations. The recent works of Vollmert and Stutz[6] concerning the determination of interpenetration through crosslinking efficiency, and of Harget and Aharoni[7] involving small-angle x-ray scattering (SAXS) and its relation with small-angle neutron scattering (SANS), both seem to corroborate our proposed model. The existence in the melt of a measurable amount of parallel-chains "bundles" was recently demonstrated by Zachmann[8] through the analysis of NMR line shape.

The Gaussian model led to crystallization theories in which each segment is deposited on a growth face after its neighbor. These theories lead to the prediction that under large supercooling the crystal thickness will increase sharply, contrary to all experimental observations. Also, these theories produce thermodynamically controlled molecular weight segregation equations that yield far poorer segregation efficiency than is actually observed.

A theory of "macromolecular nucleation" was recently put forth and corroborated by Wunderlich[9,10] which is in contrast with the common crystallization theories but lends itself to an excellent fit to the macromolecular domain concept. Wunderlich's model leaves, however, open the question of how a macromolecule becomes sufficiently ordered to be accepted into the growing crystal.

In this paper we shall first present the "amorphous" macromolecular domain and then indicate how it undergoes the process of crystallization to become eventually an integral part of the polymeric crystal or lamella.

THE AMORPHOUS MACROMOLECULAR DOMAIN

The existence of amorphous macromolecular domains ("nodules" or "globules") in crystallizable and in uncrystallizable bulk polymers is an undisputable fact proven again and again by techniques such as electron microscopy (EM) and small-angle x-ray scattering (SAXS). We believe that the present inability to detect amorphous domains in highly crystalline polymers arises from the very intense scattering of the crystalline elements, completely overshadowing the very faint amorphous scattering in techniques such as SAXS.

From the above, it becomes evident that a theory of crystallization from the melt or not-very-dilute solution must start from the macromolecular domain and not from a macromolecular chain freely floating in a neutral medium, as is assumed in the prevalent crystallization theories.

We start by defining the amorphous macromolecular domain and its internal and surface free energies. Inscribing a sphere or cylinder with a diameter b around the center of each segment, we define the segment belonging to the interior of the domain as one whose distance from all its nearest neighbors is $d \leqslant b$. Segments belonging to the matrix out of the domain do not have all their nearest neighbors at $d \leqslant b$, but some are at $d > b$. Segments comprising the domain–matrix interface belong to two half-spaces: in the interior half-space, all $d \leqslant b$; and in the exterior half-space, some $d \leqslant b$ and some $d > b$. The diameter b is taken to be about the van der Waals interaction distance.[11]

The physical cluster theory[12–15] was rigorously expanded by Stillinger[11,16] and by Lee, Baker, and Abraham.[17] This author has recently shown[18] that the physical cluster, comprised of micromolecules, can be easily replaced by a macromolecular domain, comprised of polymeric segments, while retaining the same mathematics and practically all physical parameters with the exception of T_c, the critical temperature. T_c is replaced by T_R, a reference temperature obtainable from critical-exponents equations of free volume.[19] The number of segments in the domain proper is s, with s belonging to a single molecule, several molecules, or part of a single molecule, as the case may be. The radius of the domain's interior r_1 is the distance from the domain's center of gravity to the interior point where the interfacial region begins. The radius to which the interfacial region extends is r_2.

It was shown by Stillinger[16] that the material density within a cluster is uniformly high, while the material density in the cavity (matrix) out of the cluster is uniformly low. At the interface, there is a sharp drop that can be approximated by a linear change. The same density distribution was determined theoretically to exist in and out of the amorphous macromolecular domain.[18] Experimental SAXS work of Harget and Siegmann[20] and of Harget and Aharoni,[7] with the latter correlating SAXS with small-angle neutron scattering (SANS), indicate that the segmental distribution described above actually exists in PET and PS, respectively. Accordingly,

$$\rho(r) = \rho_{pa} \qquad 0 \leqslant r \leqslant r_1 \tag{1}$$

$$\rho(r) = \rho_e + (\rho_{pa} - \rho_e)(r_2 - r)/(r_2 - r_1) \qquad r_1 \leqslant r \leqslant r_2 \tag{2}$$

$$\rho(r) = \rho_e \qquad r_2 \leqslant r \tag{3}$$

where $\rho(r)$ is the density at a point r along a ray passing through the center of gravity of the domain, ρ_{pa} is the density in the interior of the amorphous domain, and ρ_e is the density in the cavity exterior to the domain. At T_R, the interior and exterior segmental densities are equal:

$$\rho_{pa} = \rho_e = \rho_c \qquad T = T_R \tag{4}$$

where ρ_c is the average segmental density at T_R.
The ratio

$$\alpha = \rho_{pa}/(\rho_{pa} - \rho_c) \qquad \text{for } T < T_R \tag{5}$$

is an enhancement factor, always larger than unity, being the ratio of the total interior segmental density to the interior segmental density of the host domain.

At temperatures below T_R, $\rho_e \neq \rho_c$, and α undergoes slight changes; but for the present approximations these minor variations can be disregarded. The number of segments s relates the segmental density to the domain's radii:

$$s = \alpha(\pi/3)(\rho_{pa} - \rho_e)\,(r_1^3 + r_1^2 r_2 + r_1 r_2^2 + r_2^3). \tag{6}$$

Letting ΔF_a be the total free energy of an amorphous macromolecular domain, f be the homogeneous-fluid Helmholtz free energy (internal free energy) per unit volume at the respective density ρ, γ_{plane} the planar interfacial free energy, and γ_{curve} the energy correction resulting from the curvature of the domain's surface, the equation describing the free energy of a domain is

$$\begin{aligned}\Delta F_a = {} & (s/\alpha)\,(f(\rho_{pa}) - f(\rho_e))/(\rho_{pa} - \rho_e) + \\ & (s/\alpha)^{2/3} \cdot 4\pi\gamma_{\text{plane}} \cdot [(r_1 + r_2)/2]^2 \cdot (s/\alpha)^{-2/3} + \\ & (s/\alpha)^{1/3} \cdot 4\pi\gamma_{\text{curve}} \cdot [(r_1 + r_2)/2] \cdot (s/\alpha)^{-1/3} + \text{smaller terms.}\end{aligned} \tag{7}$$

A little algebra simplifies eq. (7) and reveals that ΔF_a is built from an s-dependent internal energy term and two s-independent surface energy terms:

$$\begin{aligned}\Delta F_a = {} & (s/\alpha)(f(\rho_{pa}) - f(\rho_e))/(\rho_{pa} - \rho_e) + \pi\gamma_{\text{plane}}(r_1 + r_2)^2 + \\ & 2\pi\gamma_{\text{curve}}(r_1 + r_2) + \cdots\end{aligned} \tag{8}$$

The interfacial energies above are given in terms of critical exponents:

$$\gamma_{\text{plane}} = C(T_R - T)^{1/\nu\sigma + 2\beta} = C(T_R - T)^{\mu} \tag{9}$$

and

$$\gamma_{\text{curve}} = D(T_R - T)^{2\beta} \tag{10}$$

where C and D are positive constants, σ is the compressibility exponent, μ is the surface tension exponent, and β is the critical exponent of the curve describing the coexistence of a completely uniform density on one hand and domains and cavities on the other.

THE CRYSTALLIZING MACROMOLECULAR DOMAIN

The process of crystallization from the macromolecular domain into a flat crystal or lamella is a three-step process. Initially, each domain must undergo some internal ordering, yielding a sufficient size of a reasonably well-ordered surface area. Then, and only then, domains that are sufficiently ordered can be attached onto a crystalline growth face. Highly ordered domains will serve as primary nuclei, and very disordered domains will be rejected from the growth face and remain out of the crystal. Following the step of domain attachment is the final step of regularization, which entails of attaining a uniform crystal thickness, and very often domain shape transformation aimed at minimizing the surface free energy of the attached domain and its immediate neighborhood.

We shall now follow the internal ordering and crystallization of an individual domain in some detail, using the amorphous domain's free-energy eq. (8) as our point of departure. Since the ratio α is very little changed upon crystallization, we shall ignore the minor changes in its size.

In general, the more disordered a system, the higher is its internal (Helmholtz) free energy above the equilibrium point of a fully ordered one. Since loops, folds, and other irregularities are in essence a measure of disorder, the larger the number of such irregularities per unit chain length, the higher will be its internal free energy. Denoting the density in the interior of the crystallized domain by ρ_{pc}, one must reach the conclusion that $f(\rho_{pc}) < f(\rho_{pa})$ and that

$$(s/\alpha)[f(\rho_{pa}) - f(\rho_e)]/(\rho_{pa} - \rho_e) > (s/\alpha)[f(\rho_{pc}) - f(\rho_e)]/(\rho_{pc} - \rho_e). \quad (11)$$

The change in the fold surface from domes to circles decreases the surface area and serves as a part of the driving force for segmental regularization. We shall neglect, however, this small area difference and let the fold surface be essentially planar. This is what occurs eventually in the well-regularized crystal. The planarity eliminates the curvature correction term in eqs. (7) and (8) and separates the planar surface energy into two free-energy terms, γ_1 being the surface free energy of the loop surfaces per unit area and γ_s being the surface free energy of the stem surface on the side of the cylindrical crystallizing domain. Because of the closeness of the loops' surfaces to the disorganized "amorphous" domain surface, which contains mostly loops and not straight stems, the γ_1 is closer in magnitude to γ_{plane}, albeit somewhat smaller. The rigidity and order of the stem surface makes γ_s much smaller:

$$\gamma_{\text{plane}} \lesssim \gamma_1 \gg \gamma_s. \quad (12)$$

Upon crystallization, the second term on the right-hand side of eq. (8) splits into two terms. The third term, the curvature correction term, vanishes altogether:

$$\pi\gamma_{\text{plane}}(r_1 + r_2)^2 + 2\pi\gamma_{\text{curve}}(r_1 + r_2) \rightarrow (2\pi r_1^2\gamma_1 + 2\pi r_1 L\gamma_s) = 2\pi r_1(r_1\gamma_1 + L\gamma_s) \quad (13)$$

where L is the stem length and is constrained by

$$\pi\gamma_{\text{plane}}(r_1 + r_2)^2 + 2\pi\gamma_{\text{curve}}(r_1 + r_2) > 2\pi r_1(r_1\gamma_1 + L\gamma_s). \tag{14}$$

The radius r_1 alone is used on the right-hand side of the inequality since it is the only one left upon crystallization. For a perfectly spherical crystalline domain, $L = 2r_1$. However, under practically all experimental conditions,

$$L > 2r_1. \tag{15}$$

As will be shown later, L is dependent on the $T_R - T = \Delta T$ temperature interval. Crystals can form, however, only at or below the maximum crystallization temperature, which is lower than T_R under atmospheric pressure.

Recalling that $f(\rho_{pc}) < f(\rho_{pa})$, that $\gamma_s \ll \gamma_1$, and that an increase in $2\pi r_1 L$ of a given domain can come only at the expense of $2\pi r_1^2$, we find that under isothermal conditions the total free energy of the crystallized domain, ΔF_c, is

$$\Delta F_c = (s/\alpha)(f(\rho_{pc}) - f(\rho_e))/(\rho_{pc} - \rho_e) + 2\pi r_1(r_1\gamma_1 + L\gamma_s) \tag{16}$$

that

$$\Delta F_c < \Delta F_a \tag{17}$$

and that the free energy released by a domain undergoing internal crystallization is

$$\Delta F_u = \Delta F_a - \Delta F_c. \tag{18}$$

This equation must hold for all crystallizing domains.

Noting that in eqs. (7), (8), and (16) the first right-hand side term, the internal free energy term, is negative, one observes immediately that these equations are essentially the same as those of Hoffman[21] and Wunderlich,[9] describing the free enthalpy of formation of a crystalline nucleus of a volume $\pi r_1^2 L$, containing s segments.

With increased molecular weight, the ratio of the domain's surface area to volume diminishes. This means that at a sufficiently high molecular weight, the internal free energy term in eqs. (8) and (16) becomes the dominant term. The change in free energy upon crystallization is, therefore, controlled mostly by the change in internal free energy, and the large amount of free energy released by the large domain serves essentially as the driving force for that domain's crystallization process. A partial parallel alignment of several stems in a large domain can easily trigger its complete ordering and spontaneous crystallization. Such an alignment is very probable in the larger domains, where these exist a sufficient number of segments and space to form and accommodate an aligned array of stems. It is much less probable in the smaller domains that do not have the large number of segments and the large internal volume required for aligning more than a few such stems. Very small molecules, whose segments are essentially all domain surface segments, are not expected to undergo an intradomain spontaneous crystallization. On the other end of the spectrum, the large domains do undergo spontaneous crystallization and serve as primary nuclei for a subsequent crystal growth. It is evident from the above that the increase in the ratio of the $f(\rho)$ term to the γ terms enhances internal ordering and serves as the main driving force for intradomain crystallization.

Denoting the volume fraction of the domain that underwent alignment and crystallization by $0 \leqslant y \leqslant 1$, one obtains the total free energy, ΔF_p, for a partially crystallized domain:

$$\Delta F_p = (s/\alpha)[y(f(\rho_{pc}) - f(\rho_e))/(\rho_{pc} - \rho_e) + (1 - y)(f(\rho_{pa}) - f(\rho_e))/(\rho_{pa} - \rho_e)] + 2\pi r_1(r_1\gamma_1 + L\gamma_s) \quad (19)$$

and

$$\Delta F_c < \Delta F_p < \Delta F_a. \quad (20)$$

The amount of disordered material on this domain's surface is variable and increases r somewhat to be $r_1 < r < r_2$; but because γ_{plane} and γ_1 are rather close, the total surface free energy will remain about the same. Therefore, the surface free energy term is left unchanged upon going from eq. (16) to eq. (19).

Until now we have dealt with the independent crystallization of an individual domain and with the driving force for such crystallization. We have found that the largest domains can crystallize practically to completion, that the smaller domains undergo only a partial ordering, and that the smallest domains do not improve significantly their internal order. Let us now direct our attention to the processes of attachment onto a growth face and of regularization, that is, to the processes of crystal growth and perfection.

As is well known, a polymer single crystal or lamella is built from molecular stems aligned, more or less, perpendicular to the flat basal fold surfaces which comprise of the loops. The stems and loops of each domain can remain organized as a cylinder, can spread out as a monolayer of stems on the growth face, or reach any state of reorganization intermediate between these two extremes. The difference between the two extremes is noticeable in experiments where single crystals are strained to rupture along or across the growth face. In instances where the domain had spread itself into a monolayer on the growth face, strands connecting the crystal fragments are seen only in fractures across the growth face, and none appears in fractures along the growth face. In instances where the domains retain, more or less, their initial shape, strands are seen traversing cracks in both directions. Both these characteristics were experimentally observed.[120,123]

Whether the domain retains its cylindricity or not, the loops of each domain are confined to the area of that domain's dome alone. They are, however, not necessarily adjacent, but reenter the stem region within the proximity of the domain's fold surface. The crystalline basal surfaces are defined, hence, as surfaces comprised of adjoining domes, each of which consists of proximal reentry folds. In the cases where the domain spreads as a monolayer on the growth face, almost all the loops are expected to be adjacent reentry loops, although larger distances of reentry, still within the extent of the particular domain, are present.

The driving force for the attachment of new domains onto the stem surfaces of the growth face is the diminution of the term $2\pi r_1 L\gamma_s$ in eqs. (13), (14), and (16), and the corresponding stem surface free energy of the growth face itself. Therefore, although an impetus for improved order and crystallization exists in the independent domain, contact with an ordered crystalline surface will enhance the rate of domain crystallization because of the loss of surface energy involved. Contact of a domain with the basal surface of a crystal will not promote crystallization of the domain or its attachment to the high free-energy fold surface.

This is because a fit in register, required for crystalline continuity, cannot occur on a stem surface and loop surface interface. Intradomain free energy reduction, also, cannot occur upon contact of the domain's stem surface with the highly energetic and relatively disordered loop surface.

Conceivably, the largest surface free-energy loss will occur if the whole surface $2\pi r_1 L$ will disappear. This actually happens to domains that pass through the growth face and become incorporated in the flat crystal or lamella. At the time of attachment, however, each attaching domain will tend to maximize the loss of its own and immediate neighborhood surface free energy. If the rate of domain deposition is very fast, the stem surface of each domain is immediately covered by the stem surfaces of subsequently deposited domains, and a maximal free-energy loss occurs. If the rate of domain deposition is sufficiently slow, the newly deposited domain undergoes deformation, changing from a cylinder where only a small fraction of the stem surface is in contact with the growth face to a layer, the extreme case of which is a monolayer of stems, deposited on the growth face. In this fashion, the largest area of stem surface, essentially $2\pi r_1 L$, is covered up with hardly any change in the area of the growth face. The surface free energy $2\pi r_1 L \gamma_s$ is reduced to practically nothing.

The attachment of domains on the growth face is preferential: domains that are partially ordered, and have at least a few aligned stems on their surface, can fit in register onto the growth face and will be accepted. Domains that are very disordered do not have a sufficient area of ordered stem surface and their disordered surface is highly energetic will be rejected as their surface cannot fit in register to a large enough area of crystalline stem surface to lower sufficiently the total free energy of the system. The disordered domains are those of lower molecular weight as in the smaller domains the ratio of internal free energy to interfacial free energy is small and the free energy released upon internal regularization is minimal. It can be stated, therefore, that the domains are segregated into three groups: the well-ordered large domains that eventually form the primary nuclei; the less organized domains that are sufficiently ordered to be attached onto a stem surface but not organized enough to become primary nuclei; and the domains of lower molecular weight that are so disorganized that they cannot attach themselves onto an existing stem surface and are, therefore, rejected. During normal crystallization, the second kind of domain is the predominant type.

Segmental motion in the deforming domain facilitates its regularization. This is manifested by an improved fit of the domain's stem length L to the stem length of the existing crystal by a more uniform L for all the stems in the domain, and by a better packing within the domain and between each domain and its adjacent domains. It is important to reemphasize here that as long as L is about constant, the size of the loop's surfaces will not change significantly and the free-energy losses associated with attachment and regularization all arise from the free surface energy of the stem surface and from the drop in internal free energy upon enhanced ordering of the domain.

When a domain is fully crystallized in a crystalline matrix, $y = 1$ and the free energy equation of this domain is

$$\Delta F_c = (s/\alpha)(f(\rho_{pc}) - f(\rho_e))/(\rho_{pc} - \rho_e) + 2\pi r_1(r_1\gamma_1 + (1 - x)L\gamma_s);\ 0 \leqslant x \leqslant 1 \quad (21)$$

where x diminishes from unity to zero in direct proportion to the exposed stem surface. When the stem surface of the domain is considered together with the stem surface of the growth face in its immediate neighborhood, x approaches unity even faster. Since in domains that do not crystallize spontaneously only a few stems are initially aligned, their free-energy term (which is a negative term) will not be as large as the corresponding term in eq. (16). For such domains to crystallize, the term $2\pi r_1(1 - x)L\gamma_s$ must be minimized so that eq. (18) can hold. From the description, it is evident that domains too small to crystallize independently can crystallize when deposited on a stem surface; but if their $2\pi r_1 L$ surface is disordered, they will not crystallize and be rejected from the growing crystal. It is obvious that the diminution of stem surface free energy reduces the total free energy of the domain and increases its stability. A crystalline domain fully enclosed in a crystal matrix possesses the least free energy and is, therefore, the stablest.

In the macromolecular domain, only very few long-range inter- and intramolecular "entanglements" can hold. This is in agreement with the experimental determinations of the critical molecular weight between "entanglements," yielding for each macromolecule several hundreds of repeat units between neighboring "entanglements."[22-43a] Hence, rapid crystallization can and does take place. This ease of crystallization is unexplainable according to the prevailing theories of Gaussian intramolecular segmental density distribution and their consequential multitudinous intermolecular "entanglements."

Crystal growth occurs by deposition of whole domains on the growth face of the crystal. Such deposition can be sequential or concomitant, explaining the very fast crystal growth rates observed experimentally. The domains arrive at the growth face either fully amorphous or partially crystalline, and those that are sufficiently ordered not to be rejected forthwith undergo subsequent regularization during and after their attachment. During regularization, the domain's stems attain the length L, a uniform thickness of the whole crystal. The minimal length of L is $2r_1$, and its maximal size is the length of the fully extended chain. Had L been smaller than $2r_1$, an increase in the loop surface will occur, contrary to the thermodynamically favorable decrease. At the other extreme, stretching out a single molecule to "crystallize" in an extended configuration is again energetically unfavorable: such a single chain will have more freedom of lateral mobility than several shorter stems grouped together, and the internal, Helmholtz, free energy of the chain will increase. Also, a single extended chain has an enormously large exposed stem surface that, despite the vanishingly small loop surface, makes the stem-surface energy in eqs. (16) and (21) very large and goes against the minimization of free energy. L will, therefore, reach an intermediate size, reflecting the interplay of internal and surface free energies, and will be subjected to the temperature effects on these energies. However, as long as most of the stem surfaces in a thickening crystal are in contact with one another, the changes in the internal free energy of the participating stems will not overwhelm the surface free-energy effects. Therefore, the variations in crystal thickness would be dependent on temperature mostly through the temperature dependence of the surface free energy.

Recalling eqs. (9), (12), and (13), it is evident that

$$\gamma_1 = E(T_R - T)^\mu \tag{22}$$

and

$$\gamma_s = G(T_R - T)^{\mu} \tag{23}$$

where E and G are positive constants. The values of the respective γ drop with temperature and become zero at $T = T_R$. The γ_1 and γ_s values, and consequentially the crystal thickness, are independent of the shape of the domain. Hence, an unstable state at lower temperatures can become stable at higher temperatures; a large L, unstable at low temperatures, can turn stable at the higher temperatures. Large L at high supercooling is, therefore, not expected from our model, in agreement with experimental data but unlike the expectations of the prevailing polymer crystallization theories.[44-48]

The critical exponent for surface tension μ is dependent on the compressibility exponent σ and on the coexistence exponent β. For micromolecules it was shown[49] that below T_c, $1.00 \leqslant \sigma \leqslant 1.25$. The exponent β was found to be $^1/_3$ for both micro- and macromolecules.[50,51] Assuming that σ is also the same in both instances, one obtains, see eq. (9),

$$1.17 \cong 28/24 \leqslant \mu = {}^1/_2\,\sigma + 2\beta \leqslant 31/24 \cong 1.29. \tag{24}$$

The stem length upon crystallization at $T < T_R$ can therefore be described as a function of the dependence of the surface free energy on $T_R - T$, and will take the following common critical-exponent equation form:

$$L = 2r_1((T_R - T)/T_R)^{-\mu} + A = 2r_1/(1 - T/T_R)^{\mu} + A \tag{25}$$

where A is a shift factor typical of each system and measured in the same units as r_1. The shape of the curve $(L/2r_1)$ versus $(1 - T/T_R)$ is dependent on μ and is illustrated in Figure 1. In the figure, the curve was calculated for $\mu = 1.25$, and the fit of the experimental data onto it indicates that, for all practical purposes, $\mu = 1.25$.

The relation between a temperature change and a pressure change is best described by an equation of the type[52]

$$(\Delta T)_v = (\Delta P)_v \cdot C\,^{\circ}\mathrm{K\ cm^2/kg} \tag{26}$$

indicating that at constant volume, an increase in pressure corresponds to an increase in temperature. Inserting this in eq. (25) yields

$$L = 2r_1((T_R - (\Delta P)_v \cdot C)/T_R)^{-\mu} + A = 2r_1/(1 - (\Delta P)_v \cdot C/T_R)^{\mu} + A \tag{27}$$

with the consequential increase in L as a function of increasing pressure. The reference temperature T_R is fixed in position, in a fashion similar to T_c in the case of micromolecular substances.

The following experimental observations will serve to demonstrate the validity of our model.

EXAMPLES AND DISCUSSION

The existence of macromolecular domains was proposed and extensively documented in our previous papers.[1,2] Nodules were shown to exist in many polymers,[20,53-81] ranging in size from monomolecular domains[20,53-58] up to several hundred angstroms in diameter. Domain structures were observed also in crosslinked polymers.[82-85] Single macromolecules of several polymers were

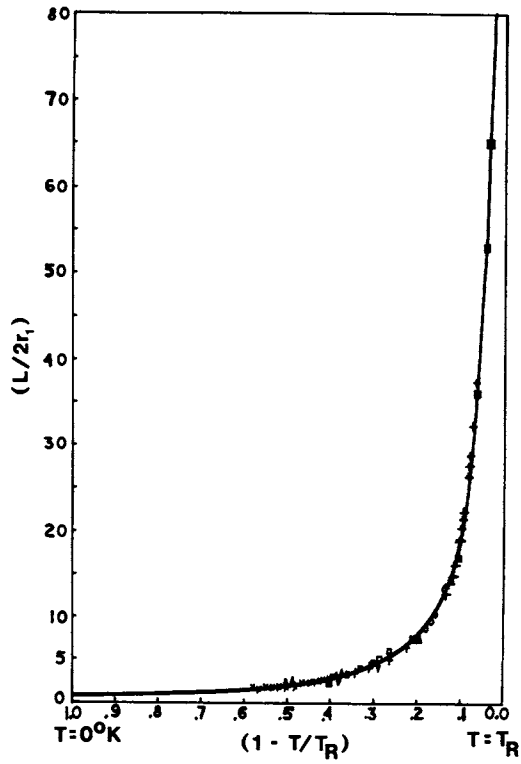

Fig. 1. Crystal thickness, represented as $L/2r_1$, plotted against $1 - (T/T_R)$. Data from references 90 and 91 for PE (○); reference 92 for PE (+); reference 93 for i-PS (×); reference 94 for i-PS (□), for POM (■), for PP (△), and for *trans*-isoprene (▽).

observed and measured, yielding an agreement between the observed and the expected volumes.[86,87]

Due to its high crystallinity and crystallization rate, it is not surprising that amorphous domains were not yet observed in conventionally prepared polyethylene (PE) samples. However, nodular structures of the order of 100 angstroms were observed in amorphous PE.[88] In another experiment, PE particles 60–100 Å in size were prepared but no crystalline diffraction pattern was obtained[89]; the failure to obtain the diffraction pattern can be attributed to the PE being in the amorphous state. The high scattering intensity of the crystalline components of polymers such as PE and polyoxymethylene (POM) masks the very weak scattering of their amorphous components and will continue to hamper the elucidation of the amorphous structure in these polymers.

Recent SAXS work of Harget and Aharoni[7] on mono- and polydispersed atactic polystyrene (PS) demonstrated the existence of molecular domains in PS and their molecular weight dependence. Correlation of these data with SANS data of PS indicates that the majority of the molecular segments are densely packed in a uniform density domain, and the remaining segments extend beyond the boundary of their domain proper. Such a distribution explains the differences between SAXS and SANS observations. Similar conclusions with respect to the segmental density distribution are arrived at on the basis of the

TABLE I
Temperature Ranges for Lamellar Thickness Determinations

Polymer	Reference no.	T_R, °K	Temperature range $(1 - T/T_R)$ Larger than	Smaller than	$2r_1$, Å	A, Å
PE	90, 91	430	0.155	0.191	15	none
PE	92	430	0.060	0.362	60	none
i-PS	93	668	0.38	0.56	35	none
i-PS	94	668	0.040	0.26	60	none
POM	94	455	0.027	0.40	very small	60
PP	94	532	0.192	0.486	20	none
trans-Isoprene	94	452	0.29	0.38	18	95

chemical crosslinking efficiency experiments recently performed by Vollmert and Stutz[6] on poly(methyl methacrylate) (PMMA).

The remarkable agreement between the theoretical eq. (25) and the experimental data is obvious from Figure 1. The data points are for PE,[90,91,92] isotactic PS,[93,94] POM,[94] PP,[94] and *trans*-isoprene.[94] The temperature ranges covered, with the resultant $2r_1$ and A values, are given in Table I.

The value of $2r_1$ for i-PS is in a reasonable agreement with the amorphous domain size of i-PS recently observed by Yeh[55,95] to be 20–50 Å in diameter. No other correlations are known to us at this time.

It was shown by Flory[96] that theories such as those of Hoffman and Lauritzen,[44,45] Frank and Tosi,[46] and Price[47,48] lead to a segmental deposition rate of $>10^{10}$ sec^{-1}. Such high rates cast doubt on the basic premises of theories assuming sequential deposition of individual segments one after the other. Recent extension of the theory by Lauritzen and Hoffman[97] and other crystallization models radically divergent in its chain folding concepts[98] hold to the notion of sequential deposition of independent segments onto the growth face.

Our model, however, facilitates high rate of segmental addition to the growth face with invoking a similar rate of deposition. In this respect, it is in agreement with Wunderlich's model.[9,10] In our case, domains ordered to different degrees can attach themselves at the same time to different points of irregularity along the same growth face and spread in either direction along the growth face. The process of attachment of partially ordered domains yields segregation according to molecular weight. This was actually observed under high pressure[99–104] and at atmospheric pressure in both melt and solution.[105–108]

Since according to our model the rate of crystallization depends on the intradomain ordering as a precondition for acceptance onto the growth face, it is the process of internal ordering that controls the growth rate and not the length of available growth face. Hence, the crystallization rate expected from our model is linear with time and is independent from the size of the growth faces. According to the common crystallization theories, the longer the growth face the higher the probability of secondary nucleation, and therefore the higher the growth rate. Since the growth face increases with time, the growth rate should increase too. This time dependence is not observed experimentally,[109] but only a linear, time-independent growth rate.

The annihilation of *ortho*-positronium in polypropylene (PP) crystals whose amorphous fold surfaces were removed by nitric acid etching showed the crystals to possess microcavities.[110] It is stated, however, that amorphous defects in the crystalline bulk are practically nonexistent.[111–113] The morphology of the crystalline surface according to our model, with the adjoining domes and the shallow channels and pits between them, explains the observations. The defects in the PE crystals and the microcavities in the acid-treated PP crystals are, most probably, deep pits formed on the surfaces at the points where more than two domes come into contact. When annealed, the deep pits can penetrate deeper into the rearranging crystal until each pair impinge upon one another and tubular slits open across the crystal thickness. NMR work[114] and the mechanical relaxation work of Sinnott[115] are in perfect agreement with the description above. The relaxation involved is the PE γ-relaxation, which has the same characteristics as the α-relaxation but appears at lower temperatures and increases in magnitude with annealing. When single crystals of PE are annealed at temperatures above their crystallization temperature while being on a coherent substrate,[116,117] they thicken and holes are formed in them. We believe that such holes are formed in the crystal at points where the domains separate from one another. Annealing PE crystals suspended in certain nonsolvents yielded similar holes in the crystals[118] leading to the same conclusions.

When POM crystals were deformed, it was observed that in some instances links exist between the crystalline fragments.[119] These links contain particulate matter about 60 Å in diameter. Periodicity of 80–100 Å was observed in drawn PE crystals[120] and bulk.[121] Links between crystalline fragments were observed in nylon 6[122] and polyacrylonitrile.[123] The observations indicate, at least in the cases of PE[120] and PAN,[123] that the fibrillar structures can appear both parallel or perpendicular to the growth face. This indicates that not in all instances a macromolecule is spread thin in a monolayer on the crystalline growth face and that multilayer remnants of domains are occasionally observed. The size of the particulate matter within the fibrillar links is independent of the thickness of the original crystals: once removed from the crystalline matrix and in no intimate contact with one another, the domains revert back to their spheroid shape.

Determinations of the amount of material in the fold regions have removed from contention both the tight adjacent reentry and the random switchboard models. It was found that the amorphous content fits a value intermediate between these two extremes,[112,113,124] but from infrared measurements[125–129a] one knows that a large number of the folds are adjacent and tight. Taking the above into consideration, Peterlin[113] calculated an average exit-to-reentry distance of 30 Å, i.e., within the dome area of each domain. The work of Keller and others on PE single crystals[130–138] involving surface etching, measurements of surface swelling, and GPC molecular weight determinations of the resultant fragments all lead to the conclusion that a smooth fold surface with tight and adjacent reentry are not in full agreement with the experimental data. Molecular weight distribution of about 15% in the degradation products, significantly broader than the instrumental distribution, indicates that there exists a distribution of accessible stem lengths within the crystal. Combining this with the fold surface being intermediate between a random switchboard model and an adjacent reentry model, one arrives at the conclusion that the adjacent domes with the proximal reentry folds model can account for all the experimental observations.

References

1. S. M. Aharoni, *J. Macromol. Sci.-Phys.*, **B7**, 73 (1973).
2. S. M. Aharoni, *J. Appl. Polym. Sci.*, **17**, 1507 (1973).
3. S. Onogi, T. Kobayashi, Y. Kojima, and Y. Taniguchi, *J. Appl. Polym. Sci.*, **7**, 847 (1963).
4. S. Onogi, T. Masuda, N. Miyanaga, and Y. Kimura, *J. Polym. Sci. A-2*, **5**, 899 (1967).
5. P. H. Lindenmeyer, *J. Macromol. Sci.-Phys.*, **B8**, 361 (1973).
6. B. Vollmert and H. Stutz, *Angew. Makromol. Chem.*, **35**, 75 (1974).
7. P. J. Harget and S. M. Aharoni, *Polym. Prepr.*, **15**(2), 39 (1974).
8. H. G. Zachmann, *Kolloid Z.Z. Polym.*, **251**, 951 (1973).
9. B. Wunderlich and A. Mehta, *J. Polym. Sci. Polym. Phys. Ed.*, **12**, 255 (1974).
10. B. Wunderlich, *Bull. Amer. Phys. Soc. Ser. II*, **19**(3), 216 (1974).
11. F. H. Stillinger, Jr., *J. Chem. Phys.*, **38**, 1486 (1963).
12. J. Frenkel, *J. Chem. Phys.*, **7**, 200 (1939).
13. W. Band, *J. Chem. Phys.*, **7**, 324 (1939).
14. J. Frenkel, *J. Chem. Phys.*, **7**, 538 (1939).
15. W. Band, *J. Chem. Phys.*, **7**, 927 (1939).
16. F. H. Stillinger, Jr., *J. Chem. Phys.*, **47**, 2513 (1967).
17. J. K. Lee, J. A. Barker, and F. F. Abraham, *J. Chem. Phys.*, **58**, 3166 (1973).
18. S. M. Aharoni, *J. Macromol. Sci.-Phys.*, **B10**, 663 (1975).
19. S. M. Aharoni, *J. Macromol. Sci.-Phys.*, **B9**, 699 (1974).
20. P. J. Harget and A. Siegmann, *J. Appl. Phys.*, **43**, 4357 (1972).
21. J. D. Hoffman, *SPE Trans.*, **4**, 315 (1964).
22. T. G. Fox and P. J. Flory, *J. Amer. Chem. Soc.*, **70**, 2384 (1948).
23. T. G. Fox and P. J. Flory, *J. Phys. Chem.*, **55**, 221 (1951).
24. T. G. Fox, S. Gratch, and S. Loshaek, in *Rheology, Theory and Applications*, Vol. 1, F. R. Eirich, Ed., Academic Press, New York, 1956, p. 431 ff.
25. R. L. Merker, *J. Polym. Sci.*, **22**, 353 (1956).
26. E. B. Bagley and D. C. West, *J. Appl. Phys.*, **29**, 1511 (1958).
27. M. L. Williams, *J. Appl. Phys.*, **29**, 1395 (1958).
28. N. Hirai, *J. Polym. Sci.*, **39**, 435 (1959).
29. Y. Oyanagi and M. Matsumoto, *J. Colloid Sci.*, **17**, 426 (1962).
30. F. Bueche, *Physical Properties of Polymers*, Interscience, New York, 1962, p. 76.
31. F. S. Dainton, D. M. Evans, F. E. Hoare, and T. P. Melia, *Polymer*, **3**, 286 (1962).
32. H. P. Schreiber, E. B. Bagley, and D. C. West, *Polymer*, **4**, 355 (1963).
33. F. Bueche, C. J. Coven, and B. J. Kinzig, *J. Chem. Phys.*, **39**, 128 (1963).
34. T. G. Fox and V. R. Allen, *J. Chem. Phys.*, **41**, 344 (1964).
35. J. P. Mercier, J. J. Aklonis, M. Litt, and A. V. Tobolsky, *J. Appl. Polym. Sci.*, **9**, 447 (1965).
36. R. J. Boyce, W. H. Bauer, and E. A. Collins, *Trans. Soc. Rheol.*, **10**, 545 (1966).
37. R. S. Porter and W. J. MacKnight, *Rubber Chem. Technol.*, **41**, 1 (1968).
38. G. C. Berry and T. G. Fox, *Advan. Polym. Sci.*, **5**, 261 (1968).
39. J. F. Sanders, J. D. Ferry, and R. H. Valentine, *J. Polym. Sci. A-2*, **6**, 967 (1968).
40. D. Gupta and W. C. Forsman, *Macromolecules*, **2**, 304 (1969).
41. G. Kraus and J. T. Gruver, *Trans. Soc. Rheol.*, **13**, 315 (1969).
42. R. F. Landel and R. F. Fedors. in *Mechanical Behavior of Materials*, Vol. III, Society of Materials Science, Japan, 1972, p. 496.
43. A. N. Gent and A. G. Thomas, *J. Polym. Sci. A-2*, **10**, 571 (1972).
43a. R. S. Porter and J. F. Johnson, *Chem. Rev.*, **66**, 1 (1966).
44. J. I. Lauritzen and J. D. Hoffman, *J. Res. Nat. Bur. Stand.*, **A64**, 73 (1960).
45. J. D. Hoffman and J. I. Lauritzen, *J. Res. Nat. Bur. Stand.*, **A65**, 297 (1961).
46. F. C. Frank and M. Tosi, *Proc. Roy. Soc.*, **A263**, 323 (1961).
47. F. P. Price, *J. Polym. Sci.*, **42**, 149 (1960).
48. F. P. Price, *J. Chem. Phys.*, **35**, 1884 (1961).
49. H. E. Stanley, *Introduction to Phase Transition and Critical Phenomena*, Oxford University Press, New York, 1971, p. 47.
50. S. M. Aharoni, Paper presented at the 101st Meeting of the A.C.S. Rubber Division, Boston, Mass., April 25–29, 1972.

51. S. M. Aharoni, *J. Polym. Sci. Symp. No. 42*, 795 (1973).
52. D. H. Kaelble, *Physical Chemistry of Adhesion*, Wiley-Interscience, New York, 1971, p. 235 ff.
53. T. G. F. Schoon and O. Teichmann, *Kolloid-Z.*, **197**, 35 (1964).
54. T. E. Brady and G. S. Y. Yeh, *J. Appl. Phys.*, **42**, 4622 (1971).
55. G. S. Y. Yeh, *J. Macromol. Sci.-Phys.*, **B6**, 451 (1972).
56. G. S. Y. Yeh, *J. Macromol. Sci.-Phys.*, **B6**, 465 (1972).
57. T. G. F. Schoon and G. Rieber, *Angew. Makromol. Chem.*, **23**, 43 (1972).
58. T. G. F. Schoon and G. Rieber, *Kautsch. Gummi Kunst.*, **25**, 456 (1972).
59. R. C. L. Mooney, *J. Amer. Chem. Soc.*, **63**, 2828 (1941).
60. G. I. Distler and Z. G. Pinsker, *Zh. Fiz. Khim.*, **23**, 1281 (1949).
61. G. I. Distler and Z. G. Pinsker, *Zh. Fiz. Khim.*, **24**, 1152 (1950).
62. M. Seal, *Phil. Mag.*, **5**, 78 (1960).
63. E. H. Andrews and A. N. Gent, in *The Chemistry and Physics of Rubber-Like Substances*, L. Bateman, Ed., Maclaren, London, 1963, pp. 225–247.
64. C. A. Garber and P. H. Geil, *J. Appl. Phys.*, **37**, 4034 (1966).
65. G. S. Y. Yeh and P. H. Geil, *J. Macromol. Sci.-Phys.*, **B1**, 235 (1967).
66. G. S. Y. Yeh and P. H. Geil, *J. Macromol. Sci.-Phys.*, **B1**, 251 (1967).
67. S. H. Carr, P. H. Geil, and E. Baer, *J. Macromol. Sci.-Phys.*, **B2**, 13 (1968).
68. A. Siegmann and P. H. Geil, *J. Macromol. Sci.-Phys.*, **B4**, 239 (1970).
69. A. Siegmann and P. H. Geil, *J. Macromol. Sci.-Phys.*, **B4**, 273 (1970).
70. J. Davidovits, *Bull. Inst. Text. France*, **25**, 987 (1971).
71. J. J. Klement and P. H. Geil, *J. Macromol. Sci.-Phys.*, **B5**, 505 (1971).
72. J. J. Klement and P. H. Geil, *J. Macromol. Sci.-Phys.*, **B5**, 535 (1971).
73. J. J. Klement, *J. Macromol. Sci.-Phys.*, **B6**, 31 (1972).
74. K. H. Yang and J. L. Kardos, *Bull. Amer. Phys. Soc. Ser. II*, **17**(3), 249 (1972).
75. P. K. C. Tsou and P. H. Geil, *Int. J. Polym. Mater.*, **1**, 223 (1972).
76. K. Neki and P. H. Geil, Technical Report #245, Division of Macromolecular Science, Case Western Reserve University, Cleveland, Ohio, July 1972.
77. W. Lin and E. J. Kramer, *J. Appl. Phys.*, **44**, 4288 (1973).
78. G. D. Wignall and G. W. Longman, *J. Mater. Sci.*, **8**, 1439 (1973).
79. C. E. Wilkes and M. H. Lear, *J. Macromol. Sci.-Phys.*, **B7**, 225 (1973).
80. R. E. Kesting, *J. Appl. Polym. Sci.*, **17**, 1771 (1973).
81. R. Salovey and R. C. Gebauer, *J. Appl. Polym. Sci.*, **17**, 2811 (1973).
82. E. H. Erath and R. A. Spurr, *J. Polym. Sci.*, **35**, 391 (1959).
83. E. H. Erath and M. Robinson, *J. Polym. Sci. C*, **No. 3**, 65 (1963).
84. H. P. Wohnsiedler, *J. Polym. Sci. C*, **No. 3**, 77 (1963).
85. V. Ye. Basin, L. M. Korsunskii, O. Yu. Shokalskaya, and N. V. Aleksandrov, *Vysokomol. Soedin.*, **A14**, 2085 (1972).
86. M. J. Richardson, *Proc. Royal Soc.*, **A279**, 50 (1964).
87. D. V. Quayle, *Br. Polym. J.*, **1**, 15 (1969).
88. V. A. Kargin and T. A. Koretskaya, *Vysokomol. Soedin.*, **1**, 1721 (1959).
89. H. Arai, T. Wada, and I. Kuriyama, *J. Polym. Sci. Polym. Phys. Ed.*, **11**, 2297 (1973).
90. A. Keller and A. O'Connor, *Disc. Faraday Soc.*, **25**, 114 (1958).
91. D. C. Bassett and A. Keller, *Phil. Mag.*, **7**, 1553 (1962).
92. L. Mandelkern, A. S. Posner, A. F. Diorio, and D. E. Roberts, *J. Appl. Phys.*, **32**, 1509 (1961).
93. D. H. Jones, A. J. Latham, A. Keller, and M. Girolamo, *J. Polym. Sci. Polym. Phys. Ed.*, **11**, 1759 (1973).
94. J. J. B. P. Blais and R. St. John Manley, *J. Macromol. Sci.-Phys.*, **B1**, 525 (1967).
95. G. S. Y. Yeh and S. L. Lambert, *J. Macromol. Sci.-Phys.*, **B6**, 599 (1972).
96. P. J. Flory, *J. Amer. Chem. Soc.*, **84**, 2857 (1962).
97. J. I. Lauritzen, Jr., and J. D. Hoffman, *J. Appl. Phys.*, **44**, 4340 (1973).
98. P. D. Calvert and D. R. Uhlmann, *J. Appl. Phys.*, **43**, 944 (1972).
99. F. R. Anderson, *J. Appl. Phys.*, **35**, 64 (1964).
100. F. R. Anderson, *J. Polymer Sci. C*, **No. 8**, 275 (1965).
101. P. H. Geil, F. R. Anderson, B. Wunderlich, and T. Arakawa, *J. Polym. Sci. A*, **2**, 3707 (1964).
102. D. V. Rees and D. C. Bassett, *Polym. Lett.*, **7**, 273 (1969).

103. W. G. Harland, M. M. Khadr, and R. H. Peters, *Polymer*, **13**, 13 (1972).
104. D. R. Beech, C. Booth. D. V. Dodgson, R. R. Sharpe, and J. R. S. Waring, *Polym.*, **13**, 73 (1972).
105. H. D. Keith and F. J. Padden, Jr., *J. Appl. Phys.*, **34**, 2409 (1963).
106. F. J. Padden, Jr., and H. D. Keith, *J. Appl. Phys.*, **37**, 4013 (1966).
107. P. R. Geil, *Polymer Single Crystals*, Interscience, New York, 1963, pp. 223–309.
108. P. H. Lindenmeyer and J. M. Peterson, *J. Appl. Phys.*, **39**, 4929 (1968).
109. B. Wunderlich, *Macromolecular Physics*, Vol. 2, Crystallization, Annealing, Melting, Academic Press, New York, in press.
110. A. Ogata and S. J. Tao, *J. Appl. Phys.*, **41**, 4261 (1970).
111. H. D. Keith, F. J. Padden, and R. G. Vadimsky, *J. Appl. Phys.*, **37**, 4027 (1966).
112. A. Peterlin and H. G. Zachmann, *J. Polym. Sci. C*, **No. 34**, 11 (1971).
113. A. Peterlin, *Polym. Prepr.*, **9**(2), 1113 (1968).
114. D. W. McCall, in *Molecular Dynamics and Structure of Solids*, NBS Special Publication 301, Nat. Bur. Stand., Washington, D.C., 1969, pp. 475–537.
115. K. M. Sinnott, *J. Appl. Phys.*, **37**, 3385 (1966).
116. W. O. Statton and P. H. Geil, *J. Appl. Polym. Sci.*, **3**, 357 (1960).
117. W. O. Statton, *J. Appl. Phys.*, **32**, 2332 (1961).
118. R.-J. Roe, C. Gieniewski, and R. G. Vadimsky, *J. Polym. Sci. Polym. Phys. Ed.*, **11**, 1653 (1973).
119. C. A. Garber and P. H. Geil, *Makromol. Chem.*, **113**, 246 (1968).
120. P. H. Geil, *Polymer Single Crystals*, Interscience, New York, 1963, pp. 115, 167, 444, 450–452.
121. *ibid.*, p. 433.
122. *ibid.*, p. 167.
123. J. J. Klement, M.S. Thesis, Case Institute of Technology, Cleveland, Ohio, 1967.
124. E. W. Fischer, H. Goddar, and G. F. Schmidt, *J. Polym. Sci. B*, **5**, 619 (1967).
125. J. L. Koenig and D. Witenhafer, *Makromol. Chem.*, **99**, 193 (1966).
126. T. Okada and L. Mandelkern, *J. Polym. Sci. B*, **4**, 1043 (1966).
127. J. L. Koenig and M. J. Hannon, *J. Macromol. Sci.-Phys.*, **B1**, 119 (1967).
128. J. L. Koenig and M. C. Agbotwalla, *J. Macromol. Sci.-Phys.*, **B2**, 391 (1968).
129. D. E. Witenhafer and J. L. Koenig, *J. Appl. Phys.*, **39**, 4982 (1968).
129a. J. J. White, A. U. Hasan, and W. C. Sears, *J. Macromol. Sci.-Phys.*, **B7**, 177 (1973).
130. D. J. Blundell, A. Keller, and T. M. Connor, *J. Polym. Sci. A-2*, **5**, 991 (1967).
131. D. J. Blundell, A. Keller, I. M. Ward, and I. J. Grant, *J. Polym. Sci. B*, **4**, 781 (1966).
132. F. C. Frank, I. M. Ward, and T. Williams, *J. Polym. Sci. A-2*, **6**, 1357 (1968).
133. T. Williams, D. J. Blundell, A. Keller, and I. M. Ward, *J. Polym. Sci. A-2*, **6**, 1613 (1968).
134. T. Williams, A. Keller, and I. M. Ward, *J. Polym. Sci. A-2*, **6**, 1621 (1968).
135. T. Williams, Y. Udagawa, A. Keller, and I. M. Ward, *J. Polym. Sci. A-2*, **8**, 35 (1970).
136. Y. Udagawa and A. Keller, *J. Polym. Sci. A-2*, **9**, 437 (1971).
137. A. Keller and Y. Udagawa, *J. Polym. Sci. A-2*, **10**, 221 (1972).
138. A. Keller and D. J. Priest, *J. Macromol. Sci.-Phys.*, **B2**, 479 (1968).

Received May 23, 1974
Revised October 2, 1974